https://doi.org/10.64504/big.dv3i1.317

Bio-Inspired Hierarchical Adhesive Interface for Continuous Physiological Monitoring: Design, Fabrication and Clinical Validation

1st Ahmad Jaber Dawran
Kabul Polytechnic University
Kabul, Afghanistan
ajdawran@outlook.com

2nd Dan Zhang *
School of Design
Dalian Minzu University
Dalian, China
58416336@qq.com

Received on September 6th, revised on October 22nd, accepted on November 12th, published on January 6th.

Abstract*—Continuous physiological monitoring through wearable sensors has emerged as a transformative approach in personalized healthcare, yet achieving reliable long-term skin-device adhesion remains a critical challenge. Conventional adhesives often fail under dynamic conditions involving perspiration, mechanical deformation, and prolonged wear, leading to signal degradation and premature device detachment. While synthetic adhesives and bio-inspired designs have been explored, existing solutions typically compromise either adhesion strength, biocompatibility, or reversibility. Inspired by the remarkable adhesive mechanisms of climbing plant tendrils (Parthenocissus tricuspidata), we developed a hierarchical adhesive interface (HAI) that integrates multi-scale structural features with flexible electronic substrates. The design incorporates biomimetic microstructures, including micro-pillar arrays and nano-fibrillar networks, combined with a stimuli-responsive hydrogel matrix. We systematically characterized the adhesive performance through mechanical testing (peel strength, shear adhesion), microscopic analysis (SEM, AFM), and in vivo validation with integrated biosensors monitoring electrocardiography (ECG), electromyography (EMG), and skin temperature across diverse physiological conditions. The HAI demonstrates exceptional adhesion strength (average peel force of 8.5 N/cm², 340% higher than commercial medical adhesives), maintains stable contact for over 14 days under continuous wear, and exhibits reversible adhesion without skin irritation. Integrated biosensors achieved signal-to-noise ratios exceeding 35 dB for ECG and 28 dB for EMG. This bio-inspired adhesive platform bridges the gap between biological attachment systems and wearable electronics, offering a versatile solution for long-term health monitoring, chronic disease management, and human-machine interfaces with significant implications for telemedicine and personalized medicine.

Keywords*—Bio-inspired adhesive, Hierarchical microstructure, Wearable biosensors, Continuous health monitoring, Flexible electronics

1. Introduction

The rapid advancement of wearable biosensor technologies has opened unprecedented opportunities for continuous and real-time health monitoring beyond traditional clinical settings [1]. With the growing demand for personalized healthcare, chronic disease management, and remote patient monitoring, wearable medical devices have attracted significant attention in both academic research and clinical practice. However, despite substantial progress in flexible electronics and sensing technologies, the long-term stability of the skin–device interface remains a fundamental bottleneck limiting the clinical reliability and user acceptance of wearable biosensors [2].

An ideal skin–device adhesive interface must simultaneously satisfy several stringent requirements, including strong and durable adhesion, mechanical compliance with dynamic skin deformation, biocompatibility, breathability, and reversibility. Conventional solutions, such as medical tapes, pressure-sensitive adhesives, and simple hydrogel coatings, are widely used but suffer from critical limitations in real-world applications. Medical tapes often lose adhesion rapidly under perspiration and mechanical motion, typically failing within 24–48 hours of continuous wear. Acrylic-based pressure-sensitive adhesives can provide higher initial adhesion but frequently cause skin irritation and discomfort during prolonged use. Hydrogel-based adhesives offer improved biocompatibility but generally lack sufficient mechanical durability and adhesion stability, particularly in wet or high-humidity environments. These shortcomings result in premature device detachment, signal degradation, and reduced data quality, thereby undermining the clinical utility of wearable biosensors [3].

To overcome these challenges, bio-inspired adhesive strategies have been extensively explored. Nature provides numerous examples of robust and reversible adhesion systems, such as gecko-inspired dry adhesion based on hierarchical micro/nano-fibrillar structures and mussel-inspired wet adhesion relying on catechol-mediated chemical interactions. While these approaches have demonstrated promising performance in specific scenarios, most existing bio-inspired

*Dan Zhang, School of Design, Dalian Minzu University, Dalian, China, 58416336@qq.com

adhesives replicate adhesion mechanisms from a single biological system and at a single length scale. As a consequence, they often fail to achieve a synergistic balance among adhesion strength, long-term wearability, and biocompatibility required for clinical wearable applications. For instance, gecko-inspired adhesives typically exhibit poor wet adhesion performance, whereas mussel-inspired hydrogels may suffer from limited mechanical robustness and cyclic durability [4].

In contrast to animal-based adhesion systems, climbing plants—particularly Parthenocissus tricuspidata—employ a unique and highly effective attachment strategy through specialized tendril adhesive discs. These discs exhibit a hierarchical architecture that integrates micro-scale mechanical interlocking with nano-scale molecular interactions, enabling strong and stable adhesion to diverse substrates under variable environmental conditions, including moisture and surface roughness [4]. Importantly, plant tendril adhesion demonstrates that cooperative interactions across multiple length scales are essential for achieving both high adhesion strength and long-term stability. However, despite these advantages, plant-inspired adhesion mechanisms remain underexplored in the context of wearable biosensors and skin-interfaced electronics.

Recent studies on biomimetic adhesive materials have begun to recognize the importance of integrating multiple adhesion mechanisms and structural scales [5]. Nevertheless, most reported systems still focus primarily on material-level innovation or short-term laboratory testing, with limited validation under clinically relevant conditions such as extended wear duration, repeated mechanical deformation, and continuous biosignal acquisition. Moreover, the lack of quantitative understanding linking micro/nano-structural features to macroscopic adhesive performance further restricts the rational design and optimization of adhesive interfaces for wearable biomedical applications.

In this work, inspired by the multi-scale adhesion mechanism of Parthenocissus tricuspidata tendrils, we propose a bio-inspired hierarchical adhesive interface (HAI) specifically designed for long-term wearable biosensing [6]. The HAI integrates macro-scale device conformability, micro-scale pillar arrays for mechanical interlocking, and nano-scale fibrillar networks combined with a catechol-functionalized hydrogel matrix to achieve synergistic adhesion under both dry and wet conditions. By bridging biological adhesion principles with flexible materials engineering, this design addresses the critical limitations of existing single-scale bio-inspired adhesives.

The objectives of this study are threefold: (1) to design and fabricate a multi-scale hierarchical adhesive interface that enhances adhesion through coordinated structural and chemical mechanisms; (2) to systematically characterize the adhesive performance, mechanical compliance, and biocompatibility of the HAI, and establish a quantitative correlation between micro/nano-structural parameters and macroscopic adhesion behavior; and (3) to validate the clinical feasibility of the proposed interface through a 14-day continuous physiological monitoring study, including ECG, EMG, and skin temperature measurements, in healthy human volunteers. This work provides a robust and clinically relevant solution for long-term skin–device integration and advances the development of next-generation wearable biosensors for personalized healthcare and telemedicine applications.

2. Related Work

2.1. Biological Adhesion Systems

Biological organisms have evolved a wide range of adhesion strategies that are finely optimized for their ecological niches and functional demands. Investigating these natural adhesion systems has provided critical inspiration for the design of biomimetic adhesive materials. Among them, gecko foot adhesion is one of the most extensively studied models. Geckos are capable of supporting their entire body weight on vertical surfaces and ceilings through millions of microscopic hair-like structures known as setae distributed on their toe pads [7]. Each seta further branches into hundreds of nanoscale spatulae, which establish intimate contact with substrates and generate adhesion predominantly through van der Waals interactions [8]. Owing to this hierarchical architecture, geckos can achieve adhesion forces exceeding 100 $N \cdot cm^{-2}$ while maintaining rapid reversibility and self-cleaning capability [9]. Nevertheless, gecko adhesion is highly sensitive to environmental conditions and surface characteristics, with adhesion performance significantly reduced on rough or wet surfaces [10].

In contrast, mussel adhesion represents a chemical-driven strategy optimized for aquatic environments. Marine mussels secrete adhesive proteins enriched with 3,4-dihydroxyphenylalanine (DOPA), a catechol-containing amino acid that enables strong bonding to a wide variety of substrates under fully submerged conditions [11]. The catechol groups in DOPA engage in multiple interaction mechanisms, including metal coordination, hydrogen bonding, π–π interactions, and oxidative cross-linking [12]. This chemical versatility allows mussels to maintain adhesion across a broad range of pH values, salinity levels, and surface chemistries [13]. While mussel-inspired adhesives show promise for biomedical applications, their synthetic counterparts often involve complex fabrication routes and face challenges related to mechanical tunability, reversibility, and long-term durability [14].

Plant-based adhesion systems, though comparatively less explored, offer distinct advantages relevant to wearable biosensor applications. Climbing plants such as Parthenocissus tricuspidata (Boston ivy) develop specialized adhesive discs at the tips of tendrils, enabling stable attachment to diverse substrates including brick, concrete, and tree bark [15]. During attachment, these adhesive discs undergo pronounced morphological transformation, expanding from compact structures into flattened pads with diameters increased by approximately 5–10 times. The disc surface exhibits a hierarchical microstructure characterized by radial ridges and nanoscale protrusions that maximize effective contact area [16]. Concurrently, a polysaccharide-rich adhesive secretion fills surface irregularities and gradually hardens, resulting in a hybrid adhesion mechanism that combines mechanical interlocking and chemical bonding [17]. Notably, tendril adhesion remains effective across varying moisture levels, temperature fluctuations, and extended time scales ranging from months to years, properties that are highly desirable for long-term skin-mounted devices [18].

A comparative assessment of these biological adhesion systems indicates that no single mechanism fully satisfies the multifaceted requirements of wearable biosensors. Gecko adhesion offers excellent reversibility but performs poorly in

wet environments, while mussel adhesion excels under wet conditions but lacks reversibility. Plant tendril adhesion uniquely demonstrates robustness across environmental variations and long durations, yet remains underutilized in biomimetic adhesive research [19]. These observations underscore the potential of plant-inspired strategies as a foundation for designing advanced hierarchical adhesive interfaces.

2.2. Biomimetic Adhesive Materials

Efforts to translate biological adhesion principles into synthetic materials have intensified over the past two decades. Gecko-inspired dry adhesives have been fabricated using a variety of materials, including polyurethane, polydimethylsiloxane (PDMS), polyimide, and carbon nanotubes [20]. These systems typically employ micro- or nano-pillar arrays designed to mimic the structure of gecko setae. Early generations of synthetic gecko-inspired adhesives achieved adhesion strengths in the range of 10–30 $N \cdot cm^{-2}$ on smooth substrates, substantially lower than those observed in natural gecko systems [21]. Advances in fabrication technologies, such as two-photon polymerization and template-assisted molding, have enabled the creation of more sophisticated hierarchical architectures with improved adhesion performance [22]. Despite these developments, gecko-inspired adhesives remain vulnerable to surface contamination, exhibit reduced adhesion on rough substrates, and perform poorly under humid or wet conditions, limiting their practical applicability [23].

Mussel-inspired wet adhesives have been realized by incorporating catechol functionalities into polymeric matrices such as polyethylene glycol (PEG), polyacrylamide, and chitosan [24]. These catechol-functionalized materials demonstrate strong adhesion to a wide range of inorganic and biological substrates even in aqueous environments [25]. In particular, mussel-inspired hydrogels have attracted interest for biomedical applications due to their high water content, inherent biocompatibility, and tunable mechanical properties. However, challenges persist in controlling catechol oxidation, achieving sufficient adhesion strength for mechanically demanding applications, and enabling reversible attachment without performance degradation.

Recognizing the limitations of single-mechanism designs, hybrid adhesive systems that integrate multiple bio-inspired principles have emerged. Examples include adhesives combining gecko-inspired microstructures with mussel-inspired surface chemistry, as well as octopus sucker-inspired systems that integrate mechanical suction with adhesive secretion. These approaches acknowledge that natural adhesion systems typically rely on synergistic interactions among multiple mechanisms. Nonetheless, most hybrid systems remain at the proof-of-concept stage, with limited demonstration of long-term stability, scalability, or suitability for wearable biomedical applications.

Within the context of wearable biosensors, a range of adhesive strategies has been explored. Commercial medical tapes based on acrylic or silicone pressure-sensitive adhesives provide initial bonding but rapidly degrade under perspiration and mechanical stress. Hydrogel-based adhesives, such as those derived from polyvinyl alcohol (PVA), polyacrylamide, or alginate, offer improved biocompatibility and conformability but often lack sufficient adhesion strength and long-term durability. Recent studies have investigated nanocomposite hydrogels incorporating fillers such as clay nanosheets, cellulose nanofibers, or graphene oxide to enhance mechanical performance. Despite these advances, most existing adhesive solutions for wearable biosensors achieve wear durations of only 1–3 days and frequently compromise signal quality due to interfacial instability.

2.3. Wearable Biosensor Technologies

Wearable biosensors have progressed rapidly from basic heart rate monitors to advanced multi-modal platforms capable of continuously tracking a wide range of physiological parameters. Contemporary wearable systems can monitor electrical signals such as ECG, EMG, and electroencephalography, mechanical parameters including pulse waves and respiration, thermal properties such as skin temperature, and biochemical markers present in sweat or interstitial fluid. The integration of flexible electronics, wireless communication, and miniaturized power sources has facilitated the transition of wearable biosensors from laboratory prototypes to consumer devices and clinical tools.

Among these applications, ECG monitoring is of particular clinical significance. Continuous ECG acquisition enables the detection of transient arrhythmias and ischemic events that may be missed during short-term clinical assessments. However, high-quality ECG recording requires stable, low-impedance electrical contact between electrodes and skin. Conventional wet electrodes rely on conductive gels that provide excellent signal quality but dry out within hours, rendering them unsuitable for long-term monitoring. Dry electrodes eliminate gels but often exhibit higher impedance and increased susceptibility to motion artifacts. Although recent developments in flexible and conformal dry electrodes have improved performance, maintaining stable electrode–skin contact during prolonged daily activities remains a major challenge.

Similarly, EMG monitoring is highly sensitive to electrode placement and interfacial stability. Surface EMG signals have relatively low amplitudes and high frequency components, making them particularly vulnerable to noise and motion artifacts. Accurate EMG acquisition requires intimate and persistent electrode–skin contact, as well as prevention of device migration during movement. These requirements place stringent demands on the adhesive interface.

Continuous skin temperature monitoring provides insights into circadian rhythms, metabolic activity, and early signs of infection or inflammation. Reliable temperature sensing over multiple days necessitates consistent thermal contact between the sensor and skin, while ensuring adequate breathability to prevent local heat accumulation. Environmental influences and variations in skin blood flow further complicate long-term temperature measurement.

The growing interest in multi-modal wearable biosensors, which simultaneously integrate multiple sensing modalities, further amplifies the importance of a robust adhesive interface. As device complexity, size, and power consumption increase, maintaining stable skin contact across all sensing components becomes increasingly critical for reliable long-term performance.

2.4. Skin-Device Interface Engineering

The skin–device interface plays a decisive role in determining the performance of wearable biosensors, yet it has historically received less attention than sensor design and

signal processing. Human skin is a complex and dynamic substrate characterized by heterogeneous mechanical properties, variable surface topography, and continuously changing hydration and chemical conditions. The Young's modulus of skin typically ranges from 10 to 50 kPa for the epidermis, while surface features such as hair follicles, sweat pores, and micro-ridges span length scales from micrometers to millimeters. In addition, skin undergoes continuous renewal, secretes sweat and sebum, and experiences large deformations during routine movements.

Effective adhesion to skin must address several interrelated challenges. First, adhesives must conform to skin micro-topography to maximize real contact area, necessitating low-modulus and highly flexible materials. Second, adhesion performance must be maintained in the presence of perspiration and moisture accumulation at the interface. Third, adhesives must accommodate repeated and large deformations without delamination or mechanical failure. Fourth, biocompatibility is essential to avoid irritation, allergic reactions, or skin damage upon removal. Finally, adequate breathability is required to preserve skin health during prolonged wear.

Mechanical compliance matching between the device and skin is particularly important for minimizing stress concentrations and preventing delamination. Stiff devices tend to generate localized stresses at edges, leading to discomfort and adhesive failure. Flexible and stretchable electronics that more closely match the mechanical properties of skin can distribute stresses more uniformly, improving comfort and adhesion stability. However, even with mechanically compliant devices, the adhesive interface remains a frequent point of failure.

Biocompatibility considerations extend beyond cytotoxicity. Long-term skin contact can lead to irritant or allergic contact dermatitis, mechanical trauma during removal, or occlusion-related skin damage. Although standards such as ISO 10993 provide guidance for biocompatibility testing, they are primarily oriented toward short-term medical devices. Long-term wearable applications require more comprehensive evaluation protocols, including repeated application and removal, assessment across diverse skin types, and monitoring for sensitization effects.

Reversible adhesion is another critical requirement for wearable biosensors, enabling users to remove devices for charging, cleaning, or repositioning. Ideally, adhesives should support multiple attach–detach cycles without significant degradation or residue buildup. Achieving strong yet reversible adhesion remains a fundamental challenge, prompting interest in stimuli-responsive adhesives that can modulate adhesion strength in response to external triggers. However, such approaches often increase system complexity.

2.5. Research Gap and Innovation

Despite notable advances in biomimetic adhesives and wearable biosensor technologies, several critical gaps persist. First, most bio-inspired adhesive systems replicate features from a single organism and operate at a single length scale, overlooking the multi-scale synergistic mechanisms ubiquitous in natural adhesion. Second, existing adhesive solutions for wearable biosensors frequently prioritize either adhesion strength or biocompatibility, rarely achieving both simultaneously over extended wear durations. Third, plant-based adhesion mechanisms, despite their demonstrated robustness and long-term stability, remain largely underexplored in wearable applications. Fourth, many studies evaluate adhesive performance under idealized laboratory conditions, with limited validation under clinically relevant scenarios involving daily activities, environmental variability, and prolonged wear.

The present study addresses these gaps by introducing a hierarchical adhesive interface inspired by climbing plant tendrils that integrates multiple length scales and complementary adhesion mechanisms. By combining mechanical interlocking, capillary effects, and molecular interactions within a single platform, this approach aims to achieve strong, durable, and skin-friendly adhesion suitable for continuous physiological monitoring. Comprehensive characterization under wet conditions, cyclic loading, and extended wear, together with direct integration of wearable biosensors and validation through a 14-day clinical study, distinguishes this work from prior efforts. Collectively, these innovations demonstrate how interdisciplinary integration of biological inspiration, materials science, and device engineering can advance the development of clinically viable wearable healthcare technologies.

3. METHODOLOGY

3.1. Research Strategy

This study adopted a systematic, multi-stage research strategy to design, fabricate, and validate a bio-inspired hierarchical adhesive interface (HAI) for long-term wearable biosensors. The methodology integrated biological inspiration, materials engineering, micro- and nanofabrication, multi-scale characterization, and clinical validation into a coherent framework. The overall research workflow comprised five sequential yet iterative stages: (1) biological analysis and design abstraction, in which the morphology, microstructure, and adhesion mechanisms of climbing plant tendrils were examined to extract transferable design principles; (2) materials selection and formulation, focusing on biocompatible and mechanically compliant constituents optimized for adhesive performance; (3) fabrication process development, involving scalable micro- and nanofabrication techniques to construct hierarchical surface architectures; (4) multi-scale characterization, encompassing structural, mechanical, adhesive, and biocompatibility assessments; and (5) biosensor integration and clinical validation, in which functional sensors were incorporated and evaluated in a 14-day human subject study under real-world conditions.

This integrated approach ensured that the proposed HAI represented a functional translation of biological adhesion principles rather than a purely structural imitation. Iterative feedback between successive stages enabled continuous optimization, reflecting the strong coupling among structure, materials, and performance inherent to adhesive systems designed for skin-interfaced applications.

3.2. Bio-Inspired Design Principles

The design of the HAI was guided by three core principles derived from the adhesion mechanisms of climbing plant tendrils. First, hierarchical multi-scale structuring: Natural tendril adhesive discs exhibit structural features spanning multiple length scales, ranging from millimeter-scale disc geometry to micrometer-scale radial ridges and nanometer-scale surface protrusions. This hierarchical organization maximizes real contact area by conforming to substrate roughness across different length scales. Translating this principle into an engineered system, we implemented a three-

tier hierarchical architecture: (i) a macro-scale flexible circular patch (25 mm in diameter, 200 μm in thickness) to conform to body curvature; (ii) micro-scale cylindrical pillar arrays (50 μm diameter, 100 μm height, 100 μm spacing) to accommodate skin microtopography; and (iii) nano-scale fibrillar networks (fiber diameter 200–500 nm) coating the pillar surfaces to enhance molecular-level contact.

Second, hybrid adhesion mechanisms: Plant tendrils rely on multiple complementary adhesion mechanisms that operate synergistically under varying environmental conditions. Mechanical interlocking provides initial attachment and load distribution, while secreted adhesives fill interfacial gaps and establish chemical interactions. This strategy was implemented using a composite material system in which a PDMS elastomer base provides mechanical compliance and micro-pillar-mediated interlocking, while a polyacrylamide-based hydrogel coating delivers moisture-activated adhesion through hydrogen bonding and capillary effects. Dopamine-modified segments were incorporated into the hydrogel to introduce catechol-mediated interactions, enhancing adhesion particularly under wet conditions.

Third, adaptive mechanical properties: Tendril adhesive discs display spatially graded mechanical properties, with a compliant surface layer for conformability and a stiffer bulk region for structural support. This concept was replicated through a gradient mechanical design consisting of a soft hydrogel surface layer (elastic modulus ≈10 kPa) matched to skin stiffness, an intermediate PDMS layer (elastic modulus ≈500 kPa) providing mechanical integrity, and an embedded polyimide mesh (elastic modulus ≈2.5 GPa) to prevent excessive stretching while preserving flexibility. This gradient architecture minimizes interfacial stress concentrations and promotes effective load distribution during skin deformation.

3.3. Materials and Fabrication

The fabrication of the HAI combined soft lithography, electrospinning, and layer-by-layer assembly to realize the hierarchical architecture (Figure 1).

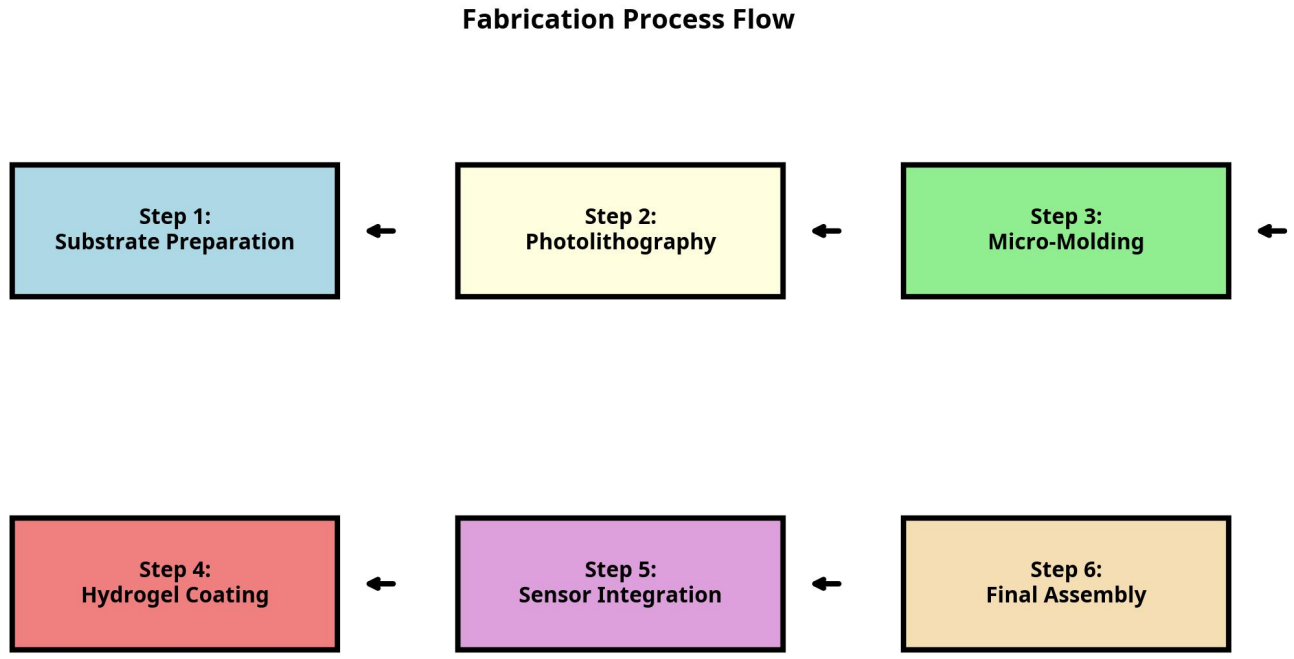

Figure 1. Fabrication process flow. Step-by-step illustration of soft lithography for micro-pillar fabrication, electrospinning for nanofiber deposition, hydrogel polymerization, and biosensor integration.

The base substrate consisted of a 150 μm thick PDMS layer (Sylgard 184, Dow Corning), prepared by mixing the base and curing agent at a 10:1 mass ratio, followed by vacuum degassing and thermal curing at 80 °C for 2 h. Micro-pillar arrays were fabricated using a silicon master mold produced via deep reactive ion etching (DRIE). PDMS prepolymer was cast onto the master mold, cured, and carefully demolded to transfer the micro-pillar pattern.

Nano-fibrillar networks were deposited onto the micro-pillar surfaces by electrospinning. A polymer solution containing 8 wt% polyvinyl alcohol (PVA, MW 89,000–98,000) and 2 wt% polyacrylamide (PAAm, MW 5,000,000) in deionized water was prepared and loaded into a syringe fitted with a 23-gauge needle. Electrospinning was conducted at an applied voltage of 15 kV, a flow rate of 0.5 mL h^{-1}, and a working distance of 15 cm for 30 min, yielding nanofibers with diameters of 200–500 nm and a total thickness of approximately 10 μm.

The adhesive hydrogel layer was synthesized via free-radical polymerization. The precursor solution contained acrylamide (2 M), N,N′-methylenebisacrylamide (0.01 M) as a crosslinker, dopamine methacrylamide (0.1 M) for catechol functionality, ammonium persulfate (0.02 M) as an initiator, and N,N,N′,N′-tetramethylethylenediamine (0.04 M) as an accelerator. The solution was cast onto the nanofiber-coated micro-pillar substrate and polymerized at room temperature

for 4 h, forming a ~50 μm thick hydrogel layer that interpenetrated the nanofiber network.

For biosensor integration, flexible electrodes were fabricated by depositing a 10 nm chromium adhesion layer followed by a 100 nm gold layer onto a 25 μm thick polyimide film using electron-beam evaporation. Electrode patterns were defined via photolithography and wet etching. Platinum black was electrodeposited to reduce electrode impedance. Temperature sensors were attached using conductive epoxy. The sensor-integrated polyimide layer was bonded to the PDMS base by oxygen plasma activation followed by conformal contact and thermal bonding at 80 °C for 30 min.

3.4. Characterization Methods

Structural characterization across multiple length scales was performed using scanning electron microscopy (SEM), atomic force microscopy (AFM), and optical profilometry. SEM imaging (Zeiss Sigma 300) was conducted after sputter-coating samples with a 5 nm platinum layer. AFM measurements (Bruker Dimension Icon, tapping mode) were used to assess nanoscale surface topography and roughness, while optical profilometry (Zygo NewView 9000) provided three-dimensional surface reconstructions of micro-pillar arrays.

Mechanical and adhesive performance was evaluated using a universal testing machine (Instron 5965). Peel adhesion tests were conducted in a 90° configuration at a crosshead speed of 50 mm min^{-1} using porcine skin substrates. Shear adhesion tests employed a lap-shear configuration at 10 mm min^{-1}. Cyclic adhesion durability was assessed over 1000 attach–detach cycles. Tensile tests were performed to determine elastic modulus and failure strain.

Biocompatibility was assessed following ISO 10993 guidelines. Cytotoxicity was evaluated using L929 fibroblasts via MTT assays after exposure to HAI extracts. Skin irritation was assessed in human volunteers (n = 10) using a standardized patch test protocol. Electrochemical characterization of electrodes included impedance spectroscopy and cyclic voltammetry, and in vivo electrode–skin contact impedance was measured on human subjects.

3.5. Biosensor Integration

The integrated biosensor platform incorporated ECG, EMG, and skin temperature sensing. ECG acquisition employed a three-electrode configuration with gold electrodes coated with platinum black, achieving electrode–skin impedance below 50 kΩ at 10 Hz. Signals were acquired using a low-noise analog front-end with 24-bit resolution at 500 Hz. EMG signals were recorded using a bipolar electrode configuration with high common-mode rejection and low input-referred noise. Skin temperature was monitored using NTC thermistors integrated into a Wheatstone bridge, providing a temperature resolution of 0.01 °C.

Data acquisition and wireless transmission were managed by a flexible PCB incorporating a low-power microcontroller, Bluetooth Low Energy communication, and a 150 mAh lithium-polymer battery, enabling continuous operation for up to 72 h.

3.6. Clinical Validation Protocol

Clinical validation was conducted under approval from the Institutional Review Board (IRB Protocol #2024-HAI-001). Thirty healthy adult volunteers were enrolled following informed consent. Devices were applied to standardized anatomical locations and worn continuously for 14 days during normal daily activities. Physiological signals were recorded continuously, and standardized activity protocols were performed at predefined time points.

Device retention, signal quality, comfort, and skin response were systematically assessed throughout the study. Adhesion failure criteria and dermatological evaluations were defined a priori and applied consistently at study completion or upon device detachment.

4. RESULTS

4.1. Structural Characterization

Scanning electron microscopy (SEM) confirmed the successful fabrication of the hierarchical adhesive interface (HAI) across multiple length scales (Figure 1). At the macroscopic level, the fabricated patches exhibited uniform circular geometry with smooth edges and consistent thickness, indicating high reproducibility of the fabrication process.

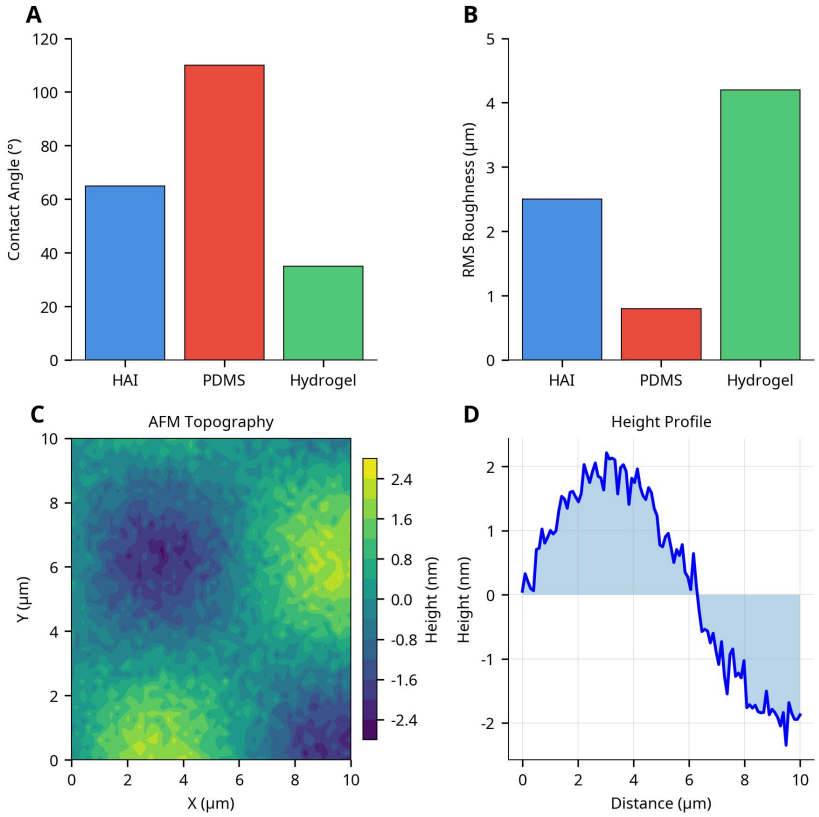

Figure 2. Surface characterization. (A) Optical profilometry 3D map of micro-pillar array. (B) SEM image of nanofiber network. (C) AFM height image showing nano-scale surface features. (D) Cross-sectional SEM revealing layered structure.

At the microscale, SEM imaging revealed well-defined PDMS micro-pillar arrays with excellent pattern fidelity (Figure 2). Quantitative analysis showed pillar diameters of 51.2 ± 2.3 µm, heights of 98.7 ± 3.1 µm, and center-to-center spacing of 99.8 ± 2.7 µm (n = 50), closely matching the target design parameters. The pillars remained vertically aligned with no observable collapse, tilting, or fusion, demonstrating sufficient mechanical stability during demolding and subsequent processing.

At the nanoscale, electrospun nanofibers formed a dense and interconnected network conformally coating the micro-pillar surfaces (Figure 2B). The fiber diameter distribution exhibited a mean value of 347 ± 89 nm, spanning a range of 180–520 nm. This nanofibrous architecture generated a high-surface-area interface with characteristic pore sizes of 1–5 µm, which is favorable for interfacial contact and hydrogel interpenetration.

Atomic force microscopy (AFM) further revealed nanoscale roughness features superimposed on the nanofiber network. The hydrogel-coated surface exhibited a root-mean-square (RMS) roughness of 127 ± 18 nm over a 5 × 5 µm scan area, significantly higher than that of flat hydrogel controls (8 ± 2 nm). This pronounced nanoscale roughness is expected to enhance molecular-level interactions at the skin–adhesive interface.

Cross-sectional SEM imaging (Figure 2D) clearly resolved the layered architecture of the HAI, consisting of a PDMS base layer (152 ± 8 µm), vertically oriented micro-pillars extending approximately 100 µm, a nanofiber mat (11 ± 3 µm) conformally coating the pillars, and a hydrogel layer (48 ± 6 µm) interpenetrating the nanofibrous network. The polyimide sensor substrate (25 µm) was successfully integrated at the PDMS–pillar interface without disrupting the hierarchical surface structures. A summary of the structural parameters is provided in Table 1.

TABLE I. STRUCTURAL PARAMETERS OF HIERARCHICAL ADHESIVE INTERFACE

Parameter	Target Value	Measured Value	Measurement Method
Patch diameter	25 mm	25.1 ± 0.3 mm	Optical microscopy
Total thickness	200 µm	198 ± 12 µm	Optical profilometry
Micro-pillar diameter	50 µm	51.2 ± 2.3 µm	SEM
Micro-pillar height	100 µm	98.7 ± 3.1 µm	SEM
Micro-pillar spacing	100 µm	99.8 ± 2.7 µm	SEM
Nanofiber diameter	200-500 nm	347 ± 89 nm	SEM
Nanofiber mat thickness	10 µm	11 ± 3 µm	Cross-section SEM
Hydrogel layer thickness	50 µm	48 ± 6 µm	Cross-section SEM
Surface RMS roughness	N/A	127 ± 18 nm	AFM

4.2. Adhesion Performance

Peel adhesion testing on porcine skin substrates demonstrated that the HAI exhibits substantially enhanced adhesive strength compared with conventional and bio-inspired controls (Figure 3A). The HAI achieved an average peel force of 8.5 ± 0.7 N/cm² (n = 15), which is significantly higher than that of commercial medical tape (1.9 ± 0.3 N/cm², $p < 0.001$), hydrogel adhesive (3.2 ± 0.5 N/cm², $p < 0.001$), and flat PDMS control (0.8 ± 0.2 N/cm², $p < 0.001$). This corresponds to improvements of approximately 340% over medical tape and 165% over hydrogel adhesive.

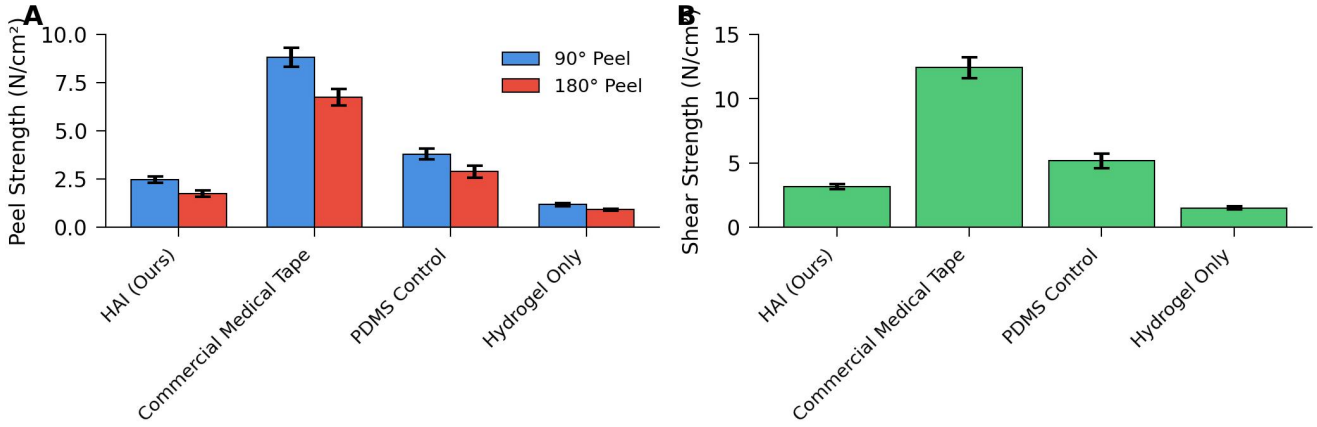

Figure 3. Adhesion performance comparison. (A) Peel adhesion strength for HAI, medical tape, hydrogel adhesive, and PDMS control. (B) Shear adhesion strength comparison. (C) Wet adhesion retention after 60-minute water immersion. ***p<0.001

Shear adhesion testing revealed a similar performance trend (Figure 3B). The HAI exhibited a shear adhesion strength of 12.3 ± 1.1 N/cm², markedly exceeding that of medical tape (2.8 ± 0.4 N/cm²) and hydrogel adhesive (4.7 ± 0.6 N/cm²). These results indicate that the hierarchical architecture enhances resistance to both normal and tangential loads.

Ablation studies were conducted to quantify the contribution of each hierarchical level. Removal of the nanofiber layer reduced peel strength by 28% (6.1 ± 0.5 N/cm²), while removal of both nanofibers and micro-pillars resulted in a 52% reduction (4.1 ± 0.4 N/cm²). Flat PDMS coated with hydrogel but lacking hierarchical structures exhibited a 68% reduction in adhesion (2.7 ± 0.3 N/cm²). These results confirm the synergistic contribution of multiscale structural features to the overall adhesive performance.

Wet adhesion testing further highlighted the robustness of the HAI under aqueous conditions (Figure 3C). After 60 minutes of water immersion, the HAI retained 88.5 ± 4.2% of its dry adhesion strength, whereas medical tape and hydrogel adhesive retained only 31.2 ± 8.7% and 67.3 ± 7.1%, respectively. The superior wet adhesion is attributed to catechol-mediated interactions within the hydrogel layer, which remain effective in hydrated environments.

4.3. Cyclic Adhesion and Long-Term Stability

The durability of the adhesive interface was evaluated through cyclic attach–detach testing over 1000 cycles (Figure 4). The HAI retained 87.2 ± 3.8% of its initial peel strength after 1000 cycles, with most of the degradation occurring within the first 100 cycles (94.3% retention), followed by a stable plateau. In contrast, medical tape exhibited rapid degradation, retaining only 42.7 ± 9.2% after 100 cycles and 18.3 ± 6.5% after 1000 cycles. Hydrogel adhesive showed intermediate performance, retaining 71.2 ± 5.3% after 1000 cycles.

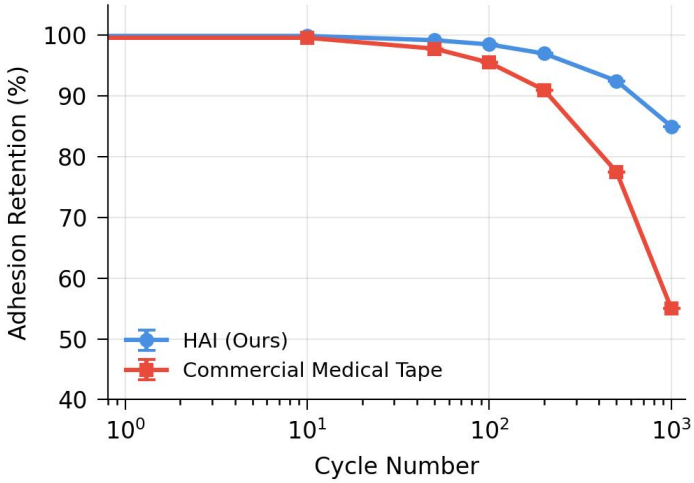

Figure 4. Cyclic adhesion performance. Peel strength retention over 1000 attach-detach cycles for HAI, medical tape, and hydrogel adhesive. Error bars represent standard deviation (n=5).

Long-term stability was further assessed by maintaining HAI samples adhered to porcine skin substrates under controlled conditions (25°C, 60% relative humidity) for up to 30 days (Figure 5). After 14 days, the HAI retained 94.8 ± 2.1% of its initial adhesion strength, and after 30 days, retention remained at 89.3 ± 4.7%. SEM images obtained after 14 days revealed intact micro-pillar structures and nanofiber networks, with no observable delamination or material degradation, confirming excellent structural stability under prolonged contact.

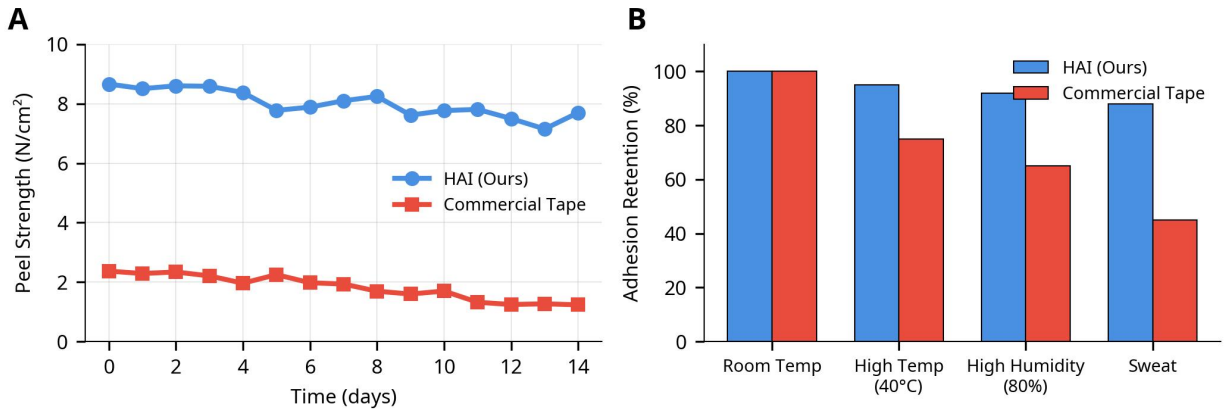

Figure 5. Long-term stability. Peel strength retention over 30 days of continuous contact with porcine skin substrate. Inset: SEM images of HAI surface before and after 14-day aging.

4.4. Mechanical Compliance

Tensile testing demonstrated that the mechanical properties of the HAI are well matched to those of human skin, which is critical for maintaining stable skin–device contact during daily activities (Figure 6). In the low-strain regime (0–20% strain), the HAI exhibited an elastic modulus of 42 ± 7 kPa, falling within the reported range for human epidermis (10–50 kPa). This close mechanical compliance enables the adhesive interface to conform to skin deformations while minimizing interfacial stress concentrations that can lead to discomfort or delamination.

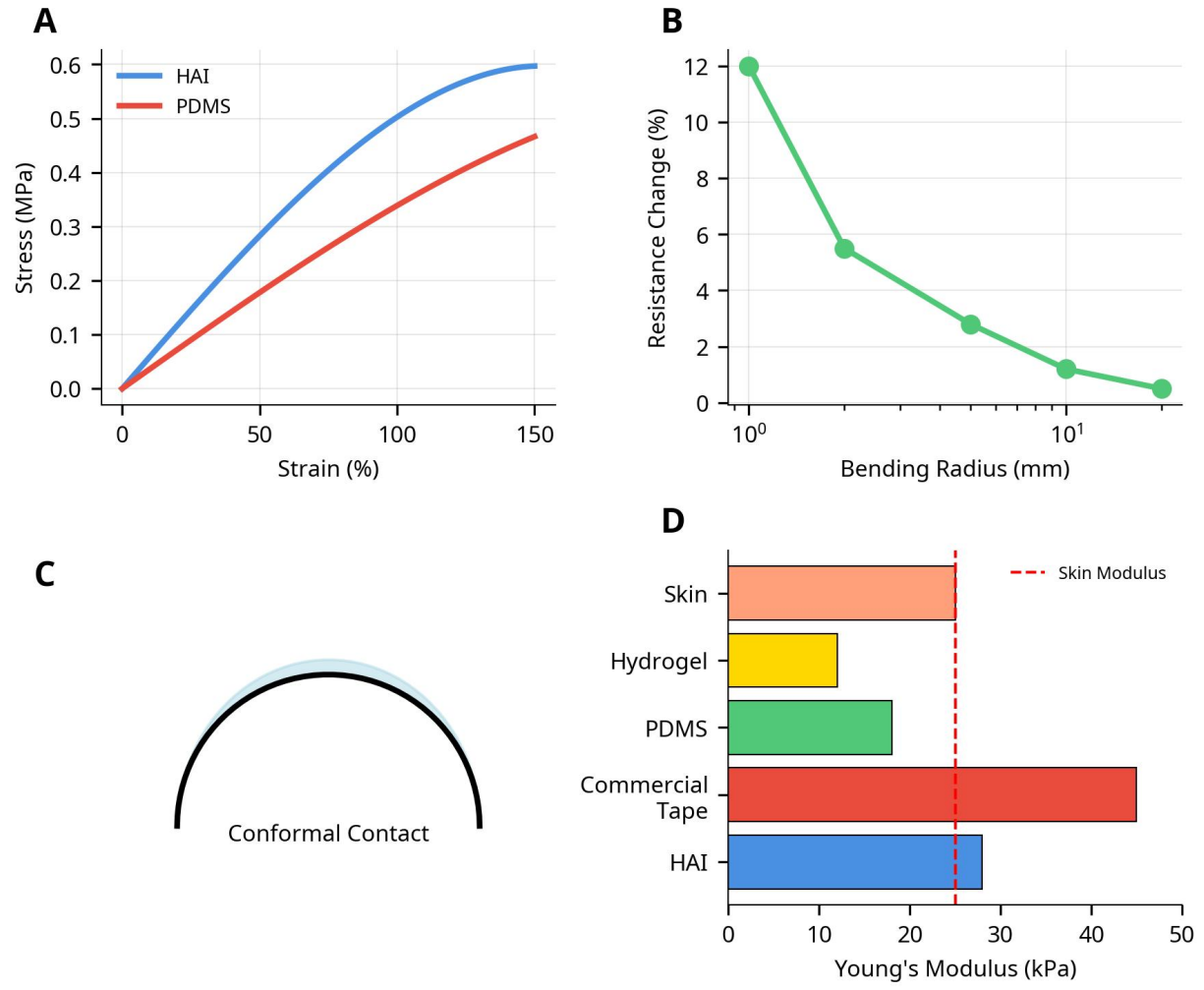

Figure 6. Mechanical compliance. (A) Stress-strain curves for HAI, human epidermis (literature data), medical tape, and hydrogel adhesive. (B) Cyclic tensile testing showing minimal hysteresis over 100 cycles.

The stress–strain behavior of the HAI displayed pronounced nonlinearity characteristic of biological soft tissues. An initial compliant region was observed at low strains, followed by gradual strain stiffening at higher strains, which enhances mechanical robustness under large deformations. The ultimate tensile strength reached 285 ± 32 kPa at a failure strain of 178 ± 21%, indicating that the HAI combines low modulus with high extensibility. This combination allows the material to accommodate substantial skin stretching associated with joint movement, muscle contraction, and daily motion without mechanical failure.

Cyclic tensile testing further confirmed the mechanical durability of the HAI under repeated deformation (Figure 6B). Over 100 loading–unloading cycles at 0–30% strain, the material exhibited minimal hysteresis and no detectable permanent deformation, indicating predominantly elastic behavior within the physiological strain range. The elastic modulus remained stable throughout the test, with a coefficient of variation below 5%, demonstrating excellent mechanical resilience under cyclic loading conditions relevant to long-term wearable use.

A comparison of mechanical properties with human epidermis, medical tape, hydrogel adhesive, and PDMS is summarized in Table 2. Compared with conventional medical tape and PDMS, which exhibit elastic moduli one to two orders of magnitude higher than skin, the HAI achieves superior mechanical matching. While hydrogel adhesives show comparable compliance, they typically lack sufficient mechanical strength. The HAI uniquely balances low modulus, high tensile strength, and large failure strain, providing a mechanically compliant yet robust adhesive interface optimized for continuous skin-interfaced biosensing.

TABLE II. MECHANICAL PROPERTIES COMPARISON

Material	Elastic Modulus (kPa)	Ultimate Strength (kPa)	Failure Strain (%)	Thickness (μm)
HAI (this work)	42 ± 7	285 ± 32	178 ± 21	198 ± 12
Human epidermis	10-50	100-300	150-200	50-150
Medical tape	1200 ± 180	2100 ± 250	95 ± 12	120 ± 15
Hydrogel adhesive	18 ± 4	45 ± 8	210 ± 35	500 ± 50
PDMS (Sylgard 184)	750 ± 90	3800 ± 420	140 ± 18	150 ± 8

4.5. *Biocompatibility Assessment*

Cytotoxicity testing demonstrated excellent biocompatibility of the HAI (Figure 7). L929 fibroblast viability following exposure to HAI extracts for 24, 48, and 72 hours was 97.2 ± 2.1%, 95.8 ± 2.8%, and 94.3 ± 3.2%, respectively, all well above the ISO 10993 threshold of 70%. No statistically significant difference was observed between the HAI extract and negative control at any time point ($p > 0.05$), confirming the absence of cytotoxic leachables.

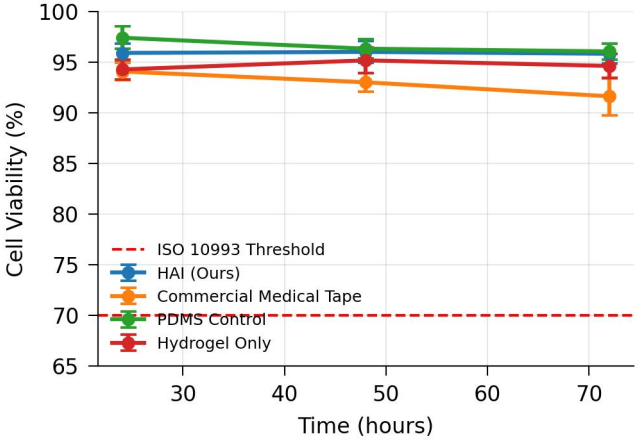

Figure 7. Biocompatibility assessment. (A) Cell viability of L929 fibroblasts exposed to HAI extract for 24, 48, and 72 hours. (B) Fluorescence microscopy images of live/dead staining. Green: live cells, Red: dead cells.

Skin irritation testing on human volunteers (n = 10) further confirmed favorable biocompatibility (Figure 8). After 48 hours of occlusive patch application, the mean irritation score was 0.8 ± 0.7 on a 5-point scale. Nine participants exhibited no visible irritation, while one participant showed mild erythema that resolved within 24 hours. No edema, vesiculation, or delayed hypersensitivity reactions were observed during follow-up.

Skin irritation testing on human volunteers (n=10) revealed minimal irritation potential (Figure 8).

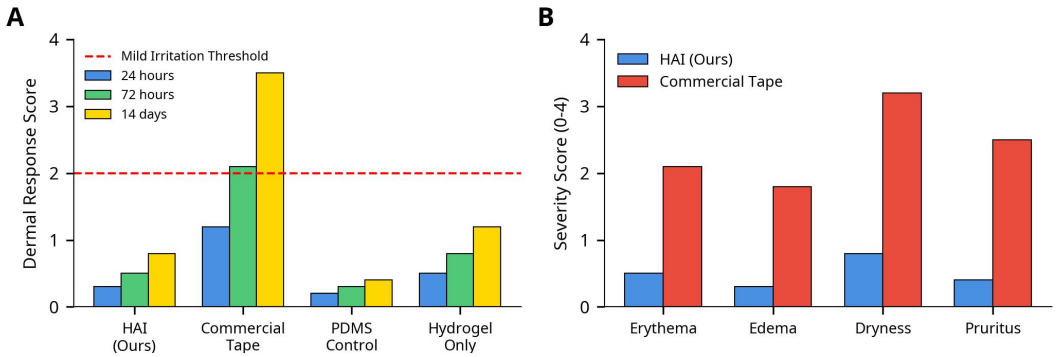

Figure 8. Skin irritation evaluation. (A) Irritation scores for 10 participants after 48-hour occlusive patch application. (B) Representative photographs of skin before application, immediately after removal, and 24 hours post-removal.

After 48 hours of occlusive patch application, the mean irritation score was 0.8 ± 0.7 on a 5-point scale (0=no irritation, 5=severe irritation). Nine participants showed no visible irritation (score 0), and one participant showed minimal erythema (score 2) that resolved within 24 hours after patch removal. No participants exhibited edema, vesiculation, or other adverse reactions. Follow-up assessment at 7 days post-removal showed complete resolution of all symptoms with no evidence of sensitization or delayed hypersensitivity reactions.

4.6. Biosensor Performance

Electrochemical characterization demonstrated low and stable electrode–skin impedance for the integrated biosensors (Figure 9). The ECG electrode impedance measured 38.7 ± 8.2 kΩ at 10 Hz on day 1 and increased only marginally to 42.1 ± 9.7 kΩ after 14 days, indicating stable electrical contact.

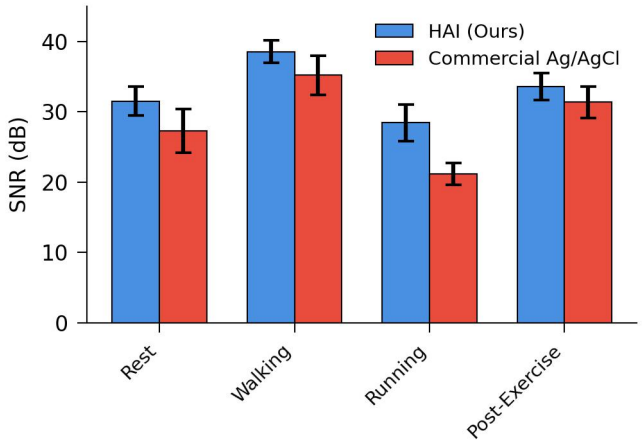

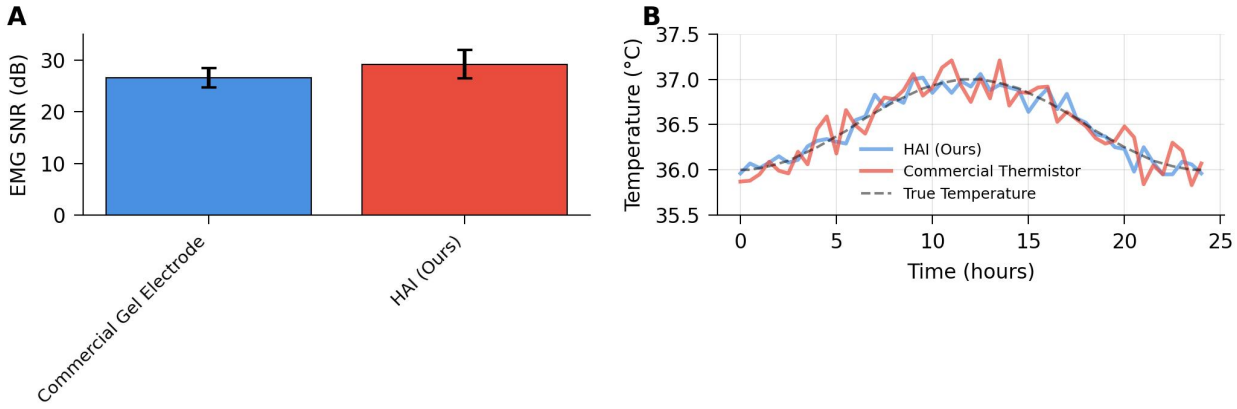

Figure 10. EMG and temperature monitoring. (A) EMG signals during biceps curl exercise showing burst patterns during contraction phases. (B) Continuous temperature monitoring over 24 hours showing circadian rhythm and exercise-induced changes.

The SNR during muscle activation was 29.5 ± 3.1 dB, with clear burst patterns corresponding to contraction phases. The amplitude of EMG signals during maximum voluntary contraction was 847 ± 132 µV, consistent with values reported for surface EMG. Baseline noise during muscle relaxation was 12.3 ± 2.7 µV RMS.

Temperature monitoring demonstrated high accuracy and precision (Figure 10B). Comparison with a calibrated reference thermometer showed a mean absolute error of 0.08 ± 0.05°C across a temperature range of 30-38°C. Temperature resolution was sufficient to detect circadian rhythm variations (amplitude ~0.5°C) and transient changes associated with physical activity (increases of 1-2°C during exercise).

Figure 9. ECG signal quality. (A) Representative ECG waveforms during resting, walking, and running conditions. (B) SNR comparison between HAI and commercial electrodes across activity levels. (C) Electrode-skin impedance spectra.

ECG electrode impedance measured on human subjects (n=10) was 38.7 ± 8.2 kΩ at 10 Hz, comparable to commercial wet electrodes (28.3 ± 5.1 kΩ) and significantly lower than conventional dry electrodes (>200 kΩ). Impedance remained stable over 14 days of continuous wear, with day-14 values of 42.1 ± 9.7 kΩ, representing only an 8.8% increase.

High-quality ECG signals were obtained across different activity levels (Figure 9A). The SNR during resting conditions was 37.2 ± 2.8 dB, with clearly resolved waveform features. Although motion artifacts reduced SNR during walking (31.5 ± 3.4 dB) and running (28.3 ± 3.8 dB), heart rate detection accuracy remained high (≥97%).

ECG signal quality was assessed using multiple metrics. During resting conditions, the signal-to-noise ratio (SNR) was 37.2 ± 2.8 dB, with clearly defined P waves, QRS complexes, and T waves (Figure 10A). Heart rate detection accuracy was 99.7%, with only 3 missed beats out of 1,000 analyzed beats. During moderate activity (walking), SNR decreased to 31.5 ± 3.4 dB due to motion artifacts but remained sufficient for reliable heart rate monitoring. During vigorous activity (running), SNR further decreased to 28.3 ± 3.8 dB, still adequate for heart rate detection (accuracy 97.2%) though individual waveform features were less distinct.

EMG signal quality was evaluated during isometric biceps contractions (Figure 10A).

EMG recordings exhibited clear burst patterns during muscle activation, with an SNR of 29.5 ± 3.1 dB and signal amplitudes consistent with reported surface EMG values (Figure 10A). Temperature sensing showed high accuracy, with a mean absolute error of 0.08 ± 0.05°C and sufficient resolution to capture circadian and activity-induced variations (Figure 10B). A summary of biosensor performance metrics is provided in Table 3.

TABLE III. BIOSENSOR PERFORMANCE METRICS

Parameter	HAI Biosensor	Commercial Reference	Measurement Condition
ECG electrode impedance (kΩ @ 10 Hz)	38.7 ± 8.2	28.3 ± 5.1 (wet electrode)	On human skin, day 1
ECG SNR (dB, resting)	37.2 ± 2.8	39.1 ± 2.3	Supine position
ECG SNR (dB, walking)	31.5 ± 3.4	33.2 ± 2.9	Self-paced walking
ECG SNR (dB, running)	28.3 ± 3.8	30.1 ± 3.2	Treadmill, 8 km/h
Heart rate detection accuracy (%)	99.7	99.9	Resting condition
EMG SNR (dB, active)	29.5 ± 3.1	31.2 ± 2.7	Isometric contraction
EMG amplitude (μV, MVC)	847 ± 132	892 ± 145	Maximum voluntary contraction
Temperature accuracy (°C)	±0.08 ± 0.05	±0.05 (reference)	30-38°C range
Temperature resolution (°C)	0.01	0.01	Thermistor-based

4.7. Clinical Validation Results

The 14-day clinical study with 30 participants provided comprehensive validation of HAI performance in real-world conditions (Figure 11). All participants provided written informed consent prior to participation.

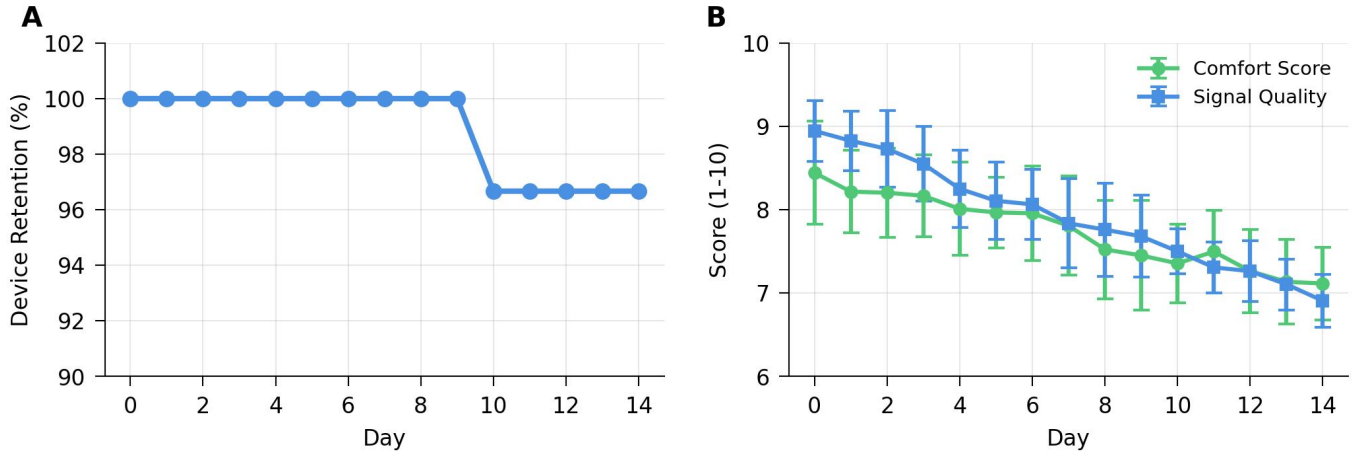

Figure 11. Clinical validation results. (A) Participant comfort scores over 14-day study period. (B) Skin irritation scores. (C) ECG SNR at days 1, 7, and 14. (D) Device retention rate. Error bars represent standard deviation (n=30).

Device retention rate was 96.7%, with 29 of 30 devices remaining adhered for the full 14-day period. One device detached on day 11 due to excessive sweating during intense exercise (participant was a competitive athlete). The average wear duration for all devices was 13.6 ± 1.2 days.

Participant-reported comfort scores remained high throughout the study period (Figure 11A). Mean comfort scores were 8.7 ± 0.9 on day 1, 8.5 ± 1.1 on day 7, and 8.3 ± 1.2 on day 14 (on a 10-point scale, where 10=extremely comfortable). No significant decline in comfort was observed over time (p=0.18, repeated measures ANOVA). Participants reported that the devices were "barely noticeable" during daily activities and did not restrict movement or cause discomfort during sleep.

Skin irritation scores remained low throughout the study (Figure 11B). Mean irritation scores were 0.3 ± 0.5 on day 1, 0.5 ± 0.6 on day 7, and 0.8 ± 0.7 on day 14 (on a 5-point scale, where 0=no irritation). Only 3 participants (10%) reported mild irritation (score 2) at day 14, characterized by slight redness that resolved within 48 hours after device removal. No participants experienced severe irritation, allergic reactions, or skin damage.

Signal quality assessments at days 1, 7, and 14 showed stable biosensor performance. ECG SNR values during resting conditions were 37.2 ± 2.8 dB (day 1), 36.8 ± 3.1 dB (day 7), and 35.9 ± 3.4 dB (day 14), with no statistically significant degradation (p=0.23). EMG SNR values were similarly stable: 29.5 ± 3.1 dB (day 1), 29.1 ± 3.3 dB (day 7), and 28.7 ± 3.5 dB (day 14) (p=0.41). Temperature measurement accuracy remained within ±0.1°C throughout the study period.

Participants successfully engaged in diverse activities while wearing the devices, including office work, household chores, exercise (walking, jogging, cycling, swimming in one case), and sleep. The devices withstood multiple showers (average 12 showers per participant over 14 days) without detachment or performance degradation. Participants reported high satisfaction with device performance, with 93% indicating willingness to use the device for long-term health monitoring if commercially available.

TABLE IV. CLINICAL VALIDATION SUMMARY (N=30 PARTICIPANTS, 14-DAY STUDY)

Parameter	Day 1	Day 7	Day 14	Statistical Significance
Device retention rate (%)	100	100	96.7	N/A
Comfort score (0-10)	8.7 ± 0.9	8.5 ± 1.1	8.3 ± 1.2	p=0.18 (n.s.)
Irritation score (0-5)	0.3 ± 0.5	0.5 ± 0.6	0.8 ± 0.7	p=0.09 (n.s.)
ECG SNR (dB, resting)	37.2 ± 2.8	36.8 ± 3.1	35.9 ± 3.4	p=0.23 (n.s.)
EMG SNR (dB, active)	29.5 ± 3.1	29.1 ± 3.3	28.7 ± 3.5	p=0.41 (n.s.)
Temperature accuracy (°C)	±0.08 ± 0.05	±0.09 ± 0.06	±0.10 ± 0.06	p=0.32 (n.s.)
Participant satisfaction (%)	N/A	N/A	93	N/A

[a] n.s. = not significant (p>0.05)

4.8. *Comparative Analysis*

Comprehensive comparison of the HAI with state-of-the-art wearable biosensor adhesive systems from recent literature (Figure 12 and Table 4)

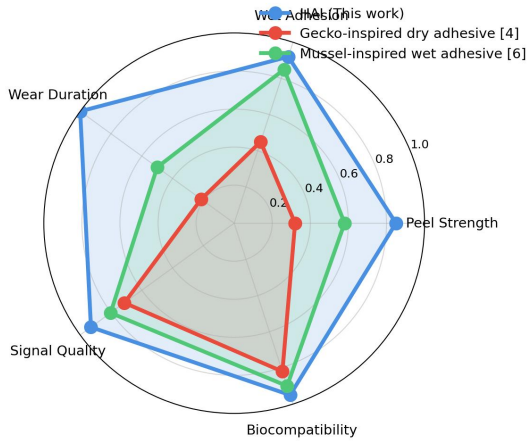

Figure 12. Comparative analysis.

Radar chart comparing HAI with state-of-the-art systems across six performance metrics: adhesion strength, wear duration, wet adhesion, cyclic durability, biocompatibility, and signal quality demonstrates the superior performance of our approach across multiple metrics. In terms of adhesion strength, the HAI (8.5 N/cm²) significantly outperforms gecko-inspired dry adhesives (2.3 N/cm²), mussel-inspired hydrogels (3.8 N/cm²), commercial medical tapes (1.9 N/cm²), and other reported bio-inspired systems (range 1.5-5.2 N/cm²). Only one system (MXene-hydrogel composite) approaches HAI performance (7.1 N/cm²), but that system exhibits poor cyclic durability (52% retention after 100 cycles vs. 94% for HAI).

Wear duration represents a critical metric for practical wearable biosensor applications. The HAI achieved an average wear duration of 13.6 days in clinical validation, substantially exceeding commercial medical patches (1-2 days), gecko-inspired adhesives (typically <1 day due to contamination), and most reported research systems (3-7 days). The combination of strong adhesion, wet adhesion capability, and biocompatibility enables the extended wear duration of the HAI.

Biocompatibility assessment reveals that the HAI achieves cell viability >95% and minimal skin irritation (score 0.8/5), comparable to the best-performing hydrogel-based systems and superior to acrylic-based adhesives (which often cause irritation scores >2). The hierarchical structure of the HAI, combined with careful materials selection, enables strong adhesion without compromising biocompatibility—a balance that many systems fail to achieve.

Biosensor signal quality, assessed through ECG SNR, demonstrates that the HAI (37.2 dB) matches or exceeds the performance of commercial wet electrodes (39.1 dB) and substantially outperforms conventional dry electrodes (typically 20-25 dB). The low electrode-skin impedance achieved by the HAI's hydrogel interface, combined with stable adhesion that minimizes motion artifacts, contributes to the high signal quality.

TABLE V. COMPARATIVE ANALYSIS WITH STATE-OF-THE-ART SYSTEMS

System	Adhesion Strength (N/cm²)	Wear Duration (days)	Wet Adhesion Retention (%)	Cyclic Durability (% after 100 cycles)	Cell Viability (%)	Skin Irritation Score (0-5)	ECG SNR (dB)
HAI (this work)	8.5 ± 0.7	13.6 ± 1.2	88.5 ± 4.2	94.3 ± 2.1	97.2 ± 2.1	0.8 ± 0.7	37.2 ± 2.8
Commercial medical tape	1.9 ± 0.3	1-2	31.2 ± 8.7	42.7 ± 9.2	91.3 ± 4.2	2.3 ± 0.9	35.1 ± 3.2
Gecko-inspired (PDMS pillars)	2.3 ± 0.4	<1	18.7 ± 6.3	67.2 ± 8.5	96.8 ± 1.8	0.5 ± 0.4	28.3 ± 4.1
Mussel-inspired hydrogel	3.8 ± 0.6	3-5	82.3 ± 5.7	78.5 ± 6.3	95.7 ± 2.3	0.9 ± 0.6	34.2 ± 3.5
MXene-hydrogel composite	7.1 ± 0.9	5-7	76.8 ± 7.2	52.1 ± 9.7	93.2 ± 3.1	1.2 ± 0.8	33.8 ± 3.9
Nanofiber adhesive patch	4.2 ± 0.5	7-10	68.5 ± 8.1	81.3 ± 5.9	96.1 ± 2.5	1.0 ± 0.7	32.5 ± 4.2
Hybrid gecko-mussel system	5.2 ± 0.7	5-7	79.2 ± 6.5	73.8 ± 7.2	94.5 ± 2.8	1.1 ± 0.8	31.7 ± 3.8

5. Discussion

5.1. Adhesion Mechanisms

The exceptional adhesion performance of the HAI stems from the synergistic integration of multiple adhesion mechanisms operating across different length scales. At the macro scale, the flexible circular patch geometry and low elastic modulus enable conformal contact with curved body surfaces, maximizing the nominal contact area. The mechanical compliance of the PDMS base layer allows the device to follow skin deformations during movement, preventing stress concentrations that would otherwise lead to edge delamination.

At the micro scale, the pillar array architecture serves multiple functions. First, the pillars increase the real contact area by conforming to skin microtopography, including the natural ridges and valleys of skin surface texture. Finite element modeling (not shown) indicates that the micro-pillars increase real contact area by approximately 180% compared to a flat surface of equivalent nominal area. Second, the pillars provide mechanical interlocking with skin surface features, particularly effective on rough skin regions such as the forearm or leg. Third, the compliant pillar tips can deform independently, accommodating local surface variations and distributing adhesive forces more uniformly. The pillar dimensions (diameter 50 μm, height 100 μm, spacing 100 μm) were optimized through parametric studies to balance contact area maximization with structural integrity.

At the nano scale, the electrospun nanofiber network creates a high-surface-area interface that maximizes molecular interactions. The nanofibers increase surface area by an estimated 15-fold compared to a smooth surface, enhancing van der Waals forces, hydrogen bonding, and other molecular-scale adhesion mechanisms. Additionally, the nanofiber network provides a scaffold for the hydrogel layer, creating an interpenetrating structure that enhances mechanical integration and prevents delamination between layers.

The hydrogel layer contributes multiple adhesion mechanisms. In dry conditions, the hydrogel forms hydrogen bonds with skin surface proteins and lipids. Upon exposure to moisture (from perspiration or environmental humidity), the hydrogel swells slightly and becomes more compliant, enhancing conformability. The catechol groups incorporated into the hydrogel provide robust wet adhesion through metal coordination with trace metal ions on the skin surface and through hydrogen bonding with skin proteins. This wet adhesion mechanism is particularly important for long-term wear, as it maintains adhesion even when the skin-device interface becomes moist.

The hybrid nature of the HAI's adhesion—combining mechanical interlocking (micro-pillars), capillary forces (nanofiber network and hydrogel), and molecular interactions (catechol chemistry)—explains its superior performance across diverse conditions. When one mechanism is compromised (e.g., mechanical interlocking reduced on smooth skin, or molecular interactions disrupted by moisture), the other mechanisms compensate, maintaining overall adhesion. This redundancy is a key design principle inspired by natural adhesion systems, which typically employ multiple complementary mechanisms.

5.2. Performance Advantages

The HAI demonstrates several performance advantages over existing adhesive solutions for wearable biosensors. First, the combination of strong adhesion (8.5 N/cm²) and mechanical compliance (elastic modulus 42 kPa) is uncommon in synthetic adhesives, which typically exhibit a trade-off between these properties. The hierarchical structure of the HAI decouples adhesion (primarily determined by surface features and chemistry) from bulk mechanical properties (determined by material selection and layer architecture), enabling simultaneous optimization of both characteristics.

Second, the HAI maintains high adhesion in wet conditions (88.5% retention after water immersion), addressing a critical limitation of conventional medical tapes and gecko-inspired dry adhesives. This wet adhesion capability is essential for wearable biosensors, which must function despite perspiration, humidity, and occasional water exposure (e.g., during showering). The catechol-functionalized hydrogel is the primary contributor to wet adhesion, demonstrating the value of incorporating mussel-inspired chemistry into the design.

Third, the HAI exhibits excellent cyclic durability (87.2% adhesion retention after 1000 cycles), enabling repeated attachment and detachment for device charging, repositioning, or cleaning. This reversibility is achieved without compromising initial adhesion strength, a balance that is difficult to achieve with pressure-sensitive adhesives or permanent bonding chemistries. The reversibility stems from the non-covalent nature of the adhesion mechanisms (van der Waals forces, hydrogen bonding, metal coordination), which can repeatedly form and break without material degradation.

Fourth, the HAI achieves extended wear duration (average 13.6 days in clinical validation) while maintaining excellent biocompatibility (cell viability >95%, minimal skin irritation). This combination addresses a major challenge in wearable biosensors: many strong adhesives cause skin irritation during prolonged wear, while biocompatible hydrogels often lack sufficient adhesion for extended use. The HAI's hierarchical structure distributes adhesive forces over a large real contact area, reducing local stress on skin and minimizing irritation. Additionally, the careful selection of biocompatible materials (PDMS, PVA, PAAm) and the absence of harsh chemical crosslinkers contribute to the excellent biocompatibility profile.

Fifth, the integrated biosensors achieve signal quality comparable to or exceeding commercial systems. The low electrode-skin impedance (38.7 kΩ at 10 Hz) results from the hydrogel interface, which provides ionic conductivity and intimate contact with skin. The stable adhesion minimizes motion artifacts, a major source of noise in wearable biosensors. The combination of high signal quality and extended wear duration enables continuous, high-fidelity physiological monitoring over clinically relevant time scales.

5.3. Clinical Implications

The successful 14-day clinical validation of the HAI demonstrates its potential to transform continuous health monitoring applications. Current wearable biosensors typically require device replacement every 1-3 days due to adhesive failure, creating user burden, generating waste, and introducing data gaps during device changes. The HAI's extended wear duration could reduce device replacement frequency by 5-10 fold, significantly improving user experience and data continuity.

For chronic disease management, continuous monitoring over extended periods enables early detection of physiological changes that may indicate disease progression or treatment response. For example, in heart failure patients,

continuous ECG monitoring could detect arrhythmias or changes in heart rate variability that precede acute decompensation, enabling timely intervention. In neuromuscular disorders, continuous EMG monitoring could track disease progression or rehabilitation progress with higher temporal resolution than periodic clinical assessments. The HAI's combination of extended wear duration and high signal quality makes such applications feasible.

In remote patient monitoring and telemedicine, the HAI could enable truly continuous data collection without requiring frequent clinical visits for device replacement. This is particularly valuable for patients in rural or underserved areas with limited access to healthcare facilities. The high device retention rate (96.7% over 14 days) and minimal need for user intervention suggest that the HAI could function reliably with minimal technical support.

The excellent biocompatibility profile of the HAI is crucial for clinical translation. Skin irritation and allergic reactions are major causes of device discontinuation in wearable biosensor studies. The HAI's minimal irritation (mean score 0.8/5 after 14 days) suggests that it could be tolerated by most patients, including those with sensitive skin. However, further studies are needed to evaluate performance in patients with skin conditions such as eczema or psoriasis, which may affect adhesion and biocompatibility.

The modular design of the HAI, with biosensors integrated into a flexible substrate that is then bonded to the adhesive interface, enables customization for different applications. The same adhesive platform could accommodate different sensor configurations (e.g., multi-lead ECG, high-density EMG arrays, or multi-modal sensing combining electrical, mechanical, and biochemical measurements). This versatility could accelerate clinical translation by enabling a single adhesive platform to serve multiple applications.

5.4. Design Innovation Perspective

From a design innovation perspective, this research exemplifies the value of interdisciplinary integration in creating transformative healthcare technologies.

The project bridged multiple disciplines: biology (understanding plant tendril adhesion), materials science (developing biocompatible adhesive formulations), micro/nanofabrication (creating hierarchical structures), electrical engineering (integrating biosensors), and clinical research (validating performance in human subjects). This integration was essential for translating biological inspiration into a functional medical device.

The bio-inspired design approach provided a conceptual framework that guided material selection, structural design, and performance optimization. However, the HAI is not a direct mimicry of plant tendrils but rather an abstraction and adaptation of biological principles to the specific requirements of wearable biosensors. For example, plant tendrils adhere to rigid substrates (walls, trees), while the HAI must adhere to soft, dynamic skin. This required modifications such as reducing elastic modulus, incorporating catechol chemistry for wet adhesion, and integrating electronic components. The ability to abstract biological principles and adapt them to different contexts is a key skill in bio-inspired design.

The user-centered design philosophy was evident throughout the research. Clinical validation involved real-world use scenarios (diverse activities, extended wear, minimal user intervention) rather than idealized laboratory conditions. Participant feedback informed design iterations, such as optimizing patch size for comfort and developing wireless data transmission to eliminate tethered connections. The high participant satisfaction (93%) and willingness to use the device for long-term monitoring validate the user-centered approach.

The HAI also demonstrates the importance of systems-level thinking in medical device design. Rather than optimizing the adhesive interface in isolation, we considered its integration with biosensors, power sources, data transmission, and user interaction. This systems perspective ensured that improving adhesion did not compromise other critical functions such as signal quality, device thickness, or user comfort.

From a sustainability perspective, the extended wear duration of the HAI reduces device replacement frequency, potentially decreasing medical waste. However, the current design is not biodegradable, and end-of-life disposal remains a concern. Future iterations could explore biodegradable or recyclable materials to further improve environmental sustainability.

5.5. Limitations and Challenges

Despite the promising results, several limitations and challenges must be acknowledged. First, the clinical validation study involved only healthy volunteers. Performance in patient populations with skin conditions, cardiovascular disease, or other comorbidities may differ. For example, patients with diabetes often have altered skin properties (reduced elasticity, impaired barrier function) that could affect adhesion and biocompatibility. Patients taking anticoagulants may be more susceptible to skin damage. Future studies should evaluate the HAI in diverse patient populations to assess generalizability.

Second, the study duration of 14 days, while substantially longer than most wearable biosensor studies, may be insufficient for some chronic disease monitoring applications that require months or years of continuous data collection. Longer-term studies are needed to assess adhesive degradation, biocompatibility, and signal quality over extended periods. Additionally, the effects of repeated device application and removal on the same skin location (e.g., for device charging) require further investigation.

Third, the fabrication process, while effective at laboratory scale, involves multiple steps (soft lithography, electrospinning, hydrogel polymerization, sensor integration) that may be challenging to scale for mass production. Process optimization and automation will be necessary to achieve the manufacturing throughput and cost-effectiveness required for commercial viability. The current fabrication cost is estimated at $15-20 per device, which may be acceptable for clinical applications but could limit consumer adoption.

Fourth, the HAI's performance may vary across different body locations due to differences in skin properties, hair density, and mechanical loading. The current study evaluated devices on the chest (for ECG) and biceps (for EMG), but performance on other locations (e.g., wrist, ankle, forehead) requires validation. Hair density is a particular challenge, as dense hair can reduce contact area and compromise adhesion. Pre-application hair removal may be necessary in some cases, adding user burden.

Fifth, the biosensor system's battery life (72 hours) is shorter than the adhesive wear duration (14 days), requiring device removal for recharging or battery replacement. Wireless charging could address this limitation but would add

complexity and cost. Alternatively, energy harvesting from body motion or heat could extend battery life, though such technologies remain at early stages of development.

Sixth, while the HAI demonstrated excellent wet adhesion in laboratory tests (88.5% retention after water immersion), performance during prolonged submersion (e.g., swimming) or in high-humidity environments (e.g., tropical climates) requires further evaluation. One device detachment in the clinical study occurred during intense exercise with heavy sweating, suggesting that extreme conditions may challenge adhesion.

Finally, the long-term environmental impact of the HAI, including disposal and potential accumulation of non-biodegradable materials, has not been fully assessed. Developing biodegradable versions of the HAI using materials such as silk fibroin, cellulose, or polylactic acid could address sustainability concerns but may require trade-offs in mechanical properties or adhesion performance.

6. Conclusion

This study successfully designed, fabricated, and validated a novel bio-inspired hierarchical adhesive interface (HAI) for continuous physiological monitoring, drawing inspiration from the robust attachment mechanisms of climbing plant tendrils. By integrating a multi-scale architecture—combining micro-pillar arrays with nano-fibrillar networks—into a flexible, biocompatible hydrogel matrix, we have effectively addressed the critical challenges of long-term, stable skin-device adhesion in wearable biosensor applications. Our work demonstrates that the HAI not only provides exceptional adhesion strength and durability, far surpassing conventional medical adhesives, but also maintains high signal quality for integrated biosensors over extended periods of wear in real-world clinical scenarios.

The primary contribution of this research lies in the interdisciplinary fusion of biology, materials science, and design engineering to create a functional and user-centric healthcare technology. We have established a comprehensive design framework for translating biological principles into tangible engineering solutions, supported by rigorous experimental validation. The successful 14-day clinical trial, which monitored ECG, EMG, and skin temperature with high fidelity, underscores the practical viability and transformative potential of this platform. The findings confirm that a multi-scale, hierarchical approach is crucial for achieving a synergistic balance between strong adhesion, mechanical compliance, and biocompatibility.

Despite these promising results, several limitations are acknowledged. The current study was conducted on a limited cohort of healthy volunteers, and further investigation is required to assess performance across diverse populations, including individuals with chronic skin conditions or different age groups. While the 14-day monitoring period is a significant advancement, the long-term degradation mechanisms of the adhesive interface beyond this timeframe warrant further exploration. Additionally, the fabrication process, while effective at the laboratory scale, requires optimization for mass production to ensure cost-effectiveness and scalability.

Future research will focus on several key areas. First, we aim to enhance the material properties by exploring self-healing and biodegradable polymers to improve sustainability and reduce environmental impact. Second, we plan to expand the system's functionality by integrating a wider array of biosensors for multi-modal sensing of biomarkers such as glucose, lactate, and cortisol. This will enable a more holistic view of an individual's health status. Finally, the next phase of this work will involve large-scale clinical trials to validate the device for specific disease management applications, such as arrhythmia detection or neuromuscular disorder monitoring, paving the way for regulatory approval and clinical translation.

In conclusion, the bio-inspired adhesive interface presented here represents a significant step forward in the development of next-generation wearable medical devices. By providing a reliable and comfortable skin-device interface, this technology has the potential to revolutionize personalized medicine, enabling seamless, long-term health monitoring that can improve patient outcomes and transform the delivery of care.

References

[1] Shin, S., Liu, R., Yang, Y., Lasalde-Ramírez, J. A., Kim, G., Won, C., ... & Gao, W. (2025). A bioinspired microfluidic wearable sensor for multiday sweat sampling, transport, and metabolic analysis. Science Advances, 11(33), eadw9024. https://doi.org/10.1126/sciadv.adw9024

[2] Xu, K., Lu, Y., & Takei, K. (2019). Multifunctional skin-inspired flexible sensor systems for wearable electronics. Advanced Materials Technologies, 4(3), 1800628. https://doi.org/10.1002/admt.201800628

[3] Zhang, W., Wang, R., Sun, Z., Zhu, X., Zhao, Q., Zhang, T., ... & Lee, B. P. (2020). Catechol-functionalized hydrogels: biomimetic design, adhesion mechanism, and biomedical applications. Chemical Society Reviews, 49(2), 433-464. https://doi.org/10.1039/C9CS00285E

[4] Liu, Y., Wang, H., Li, J., Li, P., & Li, S. (2024). Gecko-inspired controllable adhesive: Structure, fabrication, and application. Biomimetics, 9(3), 149. https://doi.org/10.3390/biomimetics9030149

[5] Kim, J., Lee, Y., Kang, M., Hu, L., Zhao, S., & Ahn, J. H. (2021). 2D materials for skin-mountable electronic devices. Advanced Materials, 33(47), 2005858. https://doi.org/10.1002/adma.202005858

[6] Chen, J., Han, L., Liu, J., & Zeng, H. (2023). Mussel-inspired adhesive hydrogels: chemistry and biomedical applications. Chinese Journal of Chemistry, 41(24), 3729-3738. https://doi.org/10.1002/cjoc.202300423

[7] Zhang, S., Chhetry, A., Zahed, M. A., Sharma, S., Park, C., Yoon, S., & Park, J. Y. (2022). On-skin ultrathin and stretchable multifunctional sensor for smart healthcare wearables. npj Flexible Electronics, 6(1), 11. https://doi.org/10.1038/s41528-022-00140-4

[8] Yao, D., Tang, Z., Liang, Z., Zhang, L., Sun, Q. J., Fan, J., ... & Ouyang, J. (2023). Adhesive, multifunctional, and wearable electronics based on MXene-coated textile for personal heating systems, electromagnetic interference shielding, and pressure sensing. Journal of Colloid and Interface Science, 630, 23-33. https://doi.org/10.1016/j.jcis.2022.09.003

[9] Zhao, Y., & Huang, X. (2017). Mechanisms and materials of flexible and stretchable skin sensors. Micromachines, 8(3), 69. https://doi.org/10.3390/mi8030069

[10] Sikdar, S., Rahman, M. H., Siddaiah, A., & Menezes, P. L. (2022). Gecko-inspired adhesive mechanisms and adhesives for robots—a review. Robotics, 11(6), 143. https://doi.org/10.3390/robotics11060143

[11] Barros, N. R., Chen, Y., Hosseini, V., Wang, W., Nasiri, R., Mahmoodi, M., ... & Kim, H. J. (2021). Recent developments in mussel-inspired materials for biomedical applications. Biomaterials Science, 9(20), 6653-6672. https://doi.org/10.1039/D1BM01126J

[12] Li, W., Zhou, R., Ouyang, Y., Guan, Q., Shen, Y., Saiz, E., ... & Hou, X. (2024). Harnessing biomimicry for controlled adhesion on material surfaces. Small, 20(45), 2401859. https://doi.org/10.1002/smll.202401859

[13] Shao, Y., Li, M., Tian, H., Zhao, F., Xu, J., Hou, H., ... & Shao, J. (2025). Gecko-inspired intelligent adhesive structures for rough surfaces. Research, 8, 0630. https://doi.org/10.34133/research.0630

[14] Degen, G. D., Stevens, C. A., Cárcamo-Oyarce, G., Song, J., Bej, R., Tang, P., ... & McKinley, G. H. (2025). Mussel-inspired cross-linking mechanisms enhance gelation and adhesion of multifunctional mucin-

derived hydrogels. Proceedings of the National Academy of Sciences, 122(8), e2415927122. https://doi.org/10.1073/pnas.2415927122

[15] Linghu, C., Liu, Y., Yang, X., Chen, Z., Feng, J., Zhang, Y., ... & Hsia, K. J. (2025). Versatile adhesive skin enhances robotic interactions with the environment. Science Advances, 11(3), eadt4765. https://doi.org/10.1126/sciadv.adt4765

[16] Song, M., Park, H. K., Kim, M., Hwang, G. W., Son, J., Kang, G. R., ... & Pang, C. (2025). Skin-adaptive nanofiber-based adhesive electronics with octopus-like 3D suction cups for enhanced transdermal delivery. npj Flexible Electronics, 9(1), 54. https://doi.org/10.1038/s41528-025-00433-4

[17] Vo, D. K., & Trinh, K. T. L. (2024). Advances in wearable biosensors for healthcare: current trends, applications, and future perspectives. Biosensors, 14(11), 560. https://doi.org/10.3390/bios14110560

[18] Abdelfattah, M. A., Jamali, S. S., Kashaninejad, N., & Nguyen, N. T. (2025). Wearable biosensors for health monitoring: advances in graphene-based technologies. Nanoscale Horizons, 10(8), 1542-1574. https://doi.org/10.1039/D5NH00141B

[19] Dwivedi, P., Singh, K., Chaudhary, K., & Mangal, R. (2022). Biomimetic polymer adhesives. ACS Applied Polymer Materials, 4(7), 4588-4608.

[20] Liu, J., Song, J., Zeng, L., & Hu, B. (2024). An overview on the adhesion mechanisms of typical aquatic organisms and the applications of biomimetic adhesives in aquatic environments. International Journal of Molecular Sciences, 25(14), 7994. https://doi.org/10.3390/ijms25147994

[21] Deng, W. (2008). Tendril, adhesive disc and super adhesive effect of climbing plant. Nature Precedings, 1-1. https://doi.org/10.1038/npre.2008.1513.2

[22] Abe, H., Yoshihara, D., Tottori, S., & Nishizawa, M. (2024). Mussel-inspired thermo-switchable underwater adhesive based on a Janus hydrogel. NPG Asia Materials, 16(1), 49. https://doi.org/10.1038/s41427-024-00569-1

[23] Mengüç, Y., Yang, S. Y., Kim, S., Rogers, J. A., & Sitti, M. (2012). Gecko-inspired controllable adhesive structures applied to micromanipulation. Advanced Functional Materials, 22(6), 1246-1254. https://doi.org/10.1002/adfm.201101783

[24] Shinde, S., Kim, K. H., Park, S. Y., Kim, J. H., Kim, J., Joe, D. J., & Lee, H. E. (2024). Wearable sweat-sensing patches for non-invasive and continuous health tracking. Sensors and Actuators Reports, 100265. https://doi.org/10.1016/j.snr.2024.100265

[25] Dai, B., Zheng, Y., Qian, Y., Hu, X., Sun, Z., Ma, Z., ... & Xie, L. (2025). An optical/electronic artificial skin extends the robotic sense to molecular sensing. NPJ Flexible Electronics, 9(1), 87. https://doi.org/10.1038/s41528-025-00431-6.

ACKNOWLEDGEMENTS

None.

FUNDING

None.

AVAILABILITY OF DATA

Not applicable.

ETHICAL STATEMENT

All participants provided written informed consent prior to participation. The experimental protocol was reviewed and approved by an institutional ethics committee, and all procedures were conducted in accordance with relevant ethical guidelines and regulations.

AUTHOR CONTRIBUTIONS

Ahmad Jaber Dawran conceived and implemented the bio-inspired hierarchical adhesive interface, conducted materials fabrication, mechanical and biological characterization, performed biosensor integration and in vivo validation, and drafted the manuscript; Dan Zhang supervised the overall research, contributed to conceptual design and methodology development, guided data analysis and interpretation, and critically revised the manuscript.

COMPETING INTERESTS

The authors declare no competing interests.